Article

Assessing the Spatiotemporal Dynamics of Vegetation Coverage in Urban Built-Up Areas

Jinlong Chen [1,2,3], Zhonglei Yu [1,2,*], Mengxia Li [1,2] and Xiao Huang [4]

1   The College of Geography and Environmental Science, Henan University, Kaifeng 475004, China
2   Key Research Institute of Yellow River Civilization and Sustainable Development, Collaborative Innovation Center on Yellow River Civilization Jointly Built by Henan Province and Ministry of Education, Henan University, Kaifeng 475001, China
3   State Key Laboratory of Information Engineering in Surveying, Mapping and Remote Sensing, Wuhan University, Wuhan 430072, China
4   Department of Geosciences, University of Arkansas, Fayetteville, AR 72701, USA
*   Correspondence: yzlei@mail.bnu.edu.cn

Abstract: As the main carbon sink in the carbon cycle process, vegetation is an important support for achieving "carbon peaking" and "carbon neutrality. How does the vegetation coverage of urban built-up areas change in the process of urbanization in China? Taking advantage of Landsat remote sensing data, we extract urban built-up areas, calculate the Normalized Difference Vegetation Index (NDVI), estimate fractional vegetation cover (FVC), and analyze the temporal and spatial dynamics of vegetation coverage in built-up areas of provincial capitals from the national and individual city levels in China. Major conclusions are as follows: (1) The FVC in the urban built-up areas has increased by 7.97%, and the urban green space has gradually changed from the "green core" distribution model to the "green vein" distribution mode. (2) The disparities in FVC of built-up areas of provincial capitals are notable, presumably due to a variety of factors that include the natural geographic environment, economic development level, built-up area expansion, land type conversion, afforestation of greening policy, etc. (3) Not just simply raise or lower, the FVC curves in the built-up areas of provincial capital cities present oscillating patterns with gradually weakening amplitude. Our study is expected to provide scientific references of an important theoretical basis for urban ecological construction and practical support for promoting the harmonious development of urban residents and urban environments in China.

Keywords: urban vegetation coverage; remote sensing; green space; urban built-up area; urbanization

1. Introduction

In the past 30 years, China's urbanization process has been characterized by its unprecedented speed and scale, and it has been at the forefront of global urbanization growth [1]. At the end of 2020, the urbanization rate of China's permanent population exceeded 60%. However, rapid urbanization led to a series of ecological and environmental pollution problems [2], e.g., air pollution, soil pollution, water resource pollution, white pollution, and heat island effect [3–5]. The growing severity of "urban disease" poses great challenges to the physical and mental health of urban residents, restricting the sustainable development of the social economy. As an important part of the urban composite ecosystem [6], urban vegetation has significant ecological service functions in the construction of the urban ecological environment [7,8]. These functions include purifying the environment [9,10], conserving water and soil [4], regulating the urban microclimate [11], alleviating the "heat island effect" [6,12,13], storing carbon confluence [14,15], and maintenance of biodiversity [16], landscape appreciation, leisure and entertainment [8], cultural education, social interaction [17], ecological protection [18], drought and disaster reduction [19]. The positive functions of urban greenness greatly benefit urban residents, as they enhance residents'

sense of happiness, relieve psychological pressure, and maintain physical and mental health [20–23]. Thus, understanding the spatiotemporal changes of the urban greenspace is a critical requirement for supporting urban planning and maintaining the function of urbanities [24]. Strengthening the construction of urban ecological greenspace and improving the quality of the living environment play an important role in urban development. At the same time, the urban vegetation ecosystem is highly affected by human factors [25], and the rapid urbanization process brings huge challenges on urban vegetation planning [10]. Better knowledge of temporal and spatial dynamics of vegetation coverage under the context of rapid urbanization is able to provide a theoretical basis and practical support for promoting the construction of urban ecological civilization and promoting the harmonious coexistence of urban residents and urban environments.

Remote sensing-based vegetation coverage estimation has become a popular approach to monitoring the quality of ecological environments [26–28]. Remote sensing data with medium spatial resolution have been widely used in monitoring the spatiotemporal dynamics of urban greenspace in response to rapid urbanization [29–31]. Numeral efforts have been made to investigate the temporal and spatial dynamics of China's long-term vegetation coverage at nationwide scale [32–35], provincial scale [36], certain urban agglomerations [37,38], and urban scales [39–41]. Studies have shown that the vegetation coverage in various regions of China presents notable spatial heterogeneity [34], and most regions have shown considerable vegetation improvement [15,32,33,35]. The impact of urbanization on vegetation differs spatially. In some regions, urbanization dominates the changes in vegetation coverage due to regional expansion [3]. Major factors that affect vegetation coverage include geographic environment, natural climate [27,32], gross domestic product (GDP) [37], human land-use changes [25,42], natural disaster such as flood, fire, etc. [43–45], afforestation of greening policy [33].

However, urban vegetation and environmental monitoring are quite different from grassland, forest, and other regional ecosystems [4]. Different vegetation environments in urban landscapes may cause slight changes, as the characteristics of vegetation landscapes in urban areas are highly heterogeneous [10]. In the existing research, the scale of world-wide and nationwide vegetation changes in time and space is too large, and the spatial resolution is too low to represent the complex process of vegetation cover changes within the city. Meanwhile, for the long-term study of urban vegetation coverage, urban administrative division maps and remote sensing data are mainly used to extract remote sensing images of the entire urban administrative area to calculate vegetation coverage [4]. The study area includes not only urban built-up areas but also other non-built-up areas, e.g., farmland, villages, and woodland, leading to large random errors and overestimated vegetation coverage. Moreover, in existing studies, the time span of remote sensing data is relatively short, and the study area is not extensive, as static data based on small samples may not accurately reflect dynamic changes to illustrate a more comprehensive understanding spatio-temporal dynamics of vegetation coverage in urban built-up areas. Finally, provincial capital cities are the political, economic, and cultural centres of the province where they are located, as the urbanization process is complete. Research on the temporal and spatial dynamics of vegetation coverage in provincial capital cities is highly representative, but in previous studies, there are few studies on the vegetation coverage of urban built-up areas at the same time for 31 provincial capital cities in mainland China.

In this study, we use urban boundary mapping of the artificial impervious surface from the global artificial impervious area, extract remote sensing images of built-up areas of provincial capital cities, calculate the normalized differential vegetation index (NDVI), estimate the fractional vegetation coverage (FVC), and evaluate the vegetation coverage and ecological environment quality of the built-up areas of provincial capitals in China. Main realizations: (1) The Spearman's rank correlation coefficient is utilized to determine the elements that influence vegetation coverage in urban built-up areas, and kernel density estimation is used to investigate the geographical distribution of vegetation coverage. (2) Making Grading maps of vegetation coverage in built-up areas of 31 provincial capital

cities from 1990 to 2020. (3) We examined the spatio-temporal dynamic of vegetation coverage in built-up areas of 31 provincial capital cities from 1990 to 2020. This study analyses the temporal and spatial evolution characteristics of vegetation coverage in built-up areas in the process of urbanization from the national and individual city levels. Our study is expected to provide scientific references of an important theoretical basis for urban ecological construction and practical support for promoting the harmonious development of urban residents and urban environments in China.

2. Materials and Methods

2.1. Study Area

We selected the built-up areas of provincial capital cities in mainland China (including municipalities and autonomous region capitals and excluding Hong Kong, Macao, and Taiwan regions) as our study area (Figure 1). In addition, it includes seven natural geographic regions divided by geographic location and climatic conditions. On the one hand, the process of urbanization is closely related to the economic foundation, industrial structure, social transformation, resources, and environment, etc. Therefore, the process of urbanization in China has significant regional differences at the provincial scale [46]. In addition, provincial capital cities are the political, economic, and cultural centers of the region, usually with high urbanization levels. The investigation of the temporal and spatial dynamics of vegetation coverage in provincial capital cities has important implications for the ecological environment construction of other cities. Provincial capital cities are geographically distributed across China in a scattered manner, basically including all types of natural endowment conditions, with varying scales, levels, and degrees of development. Such diversity benefits our understanding of different characteristics of the spatiotemporal dynamics of urban vegetation coverage throughout China in the process of urbanization.

Figure 1. The distribution of China's provincial capitals. (Map source: http://bzdt.ch.mnr.gov.cn/index.html, accessed on 1 January 2022).

2.2. Data and Pre-Processing

In this study, we use Landsat Thematic Mapper (TM) and Operational Land Imager (OLI) images with a spatial resolution of 30 m and a time resolution of 16 days as the main data sources (Data source: Geospatial Data Cloud, https://www.gscloud.cn/home, accessed on 1 January 2022). There are 263 remote sensing images and the images span

from 1990–2020 and cover 31 provincial capital cities. In order to avoid cloud interference, we choose remote sensing images with no or few clouds in the study area. At the same time, radiometric correction and atmospheric correction using ENVI software are performed on the acquired remote sensing satellite images, and image clipping and mosaicking are performed for situations where a single image fails to fully cover the urban built-up area.

We refer to an automatic delineation framework to generate a multi-temporal dataset of global urban boundaries (GUB) using 30 m global artificial impervious area (GAIA) data in seven representative years (i.e., 1990, 1995, 2000, 2005, 2010, 2015, and 2018). This dataset provides a physical boundary of urban areas that can be used to study the impact of urbanization on biodiversity, climate change, and urban health. The GUB dataset can be accessed from (http://data.ess.tsinghua.edu.cn, accessed on 1 January 2022) [47]. Furthermore, we used the global urban boundary dataset and satellite remote sensing images to manually interpret the boundary lines of the built-up areas of 31 provincial capital cities in 2020.

2.3. Methods

As shown in Figure 2, our study relies on remote sensing images of provincial capital cities in mainland China from 1990–2020 and the urban boundary dataset from the global artificial impervious surface (GAIA). We further clip remote sensing images of built-up areas in provincial capital cities and calculate the NDVI. With reference to previous research, national soil classification maps, and land use maps, we derive the NDVI confidence interval and use the dimidiate pixel model to extract the FVC in the built-up areas of provincial capital cities. Based on grading and classified statistical data, we quantitatively and visually evaluate the vegetation coverage and ecological environment quality in the built-up areas of provincial capital cities and analyze the characteristics of temporal and spatial changes and influencing factors.
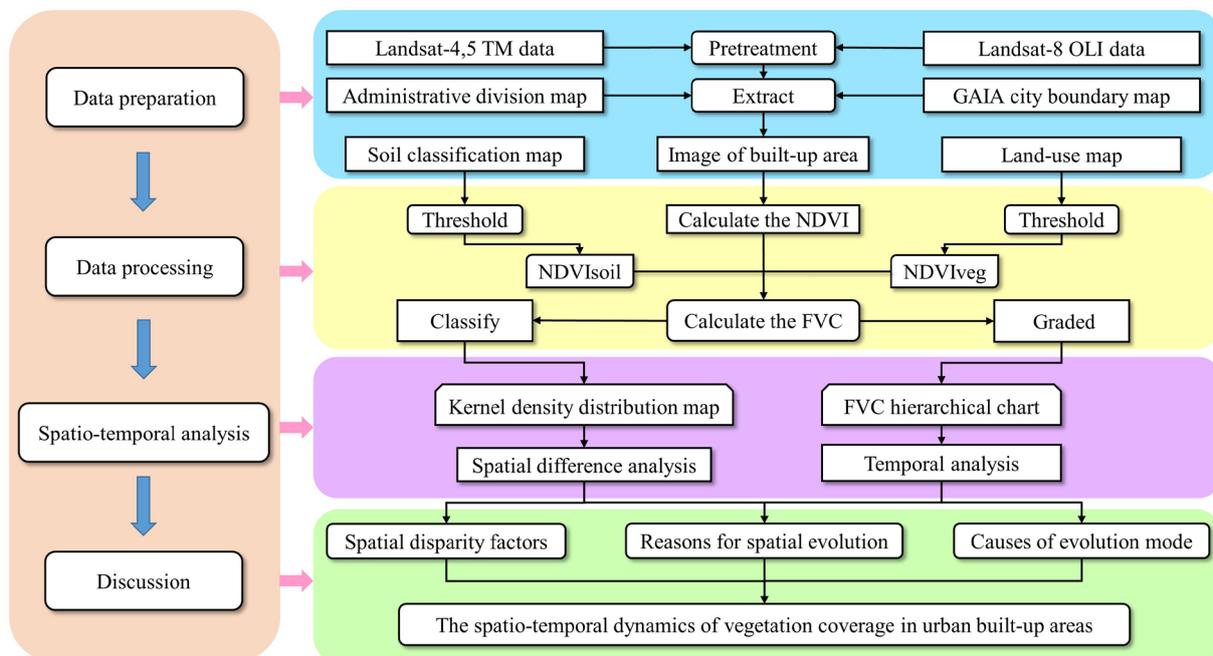

Figure 2. The general workflow of this study.

2.3.1. Fractional Vegetation Cover (FVC)

FVC refers to the percentage of the vertical projection area of vegetation (e.g., stems and leaves) on the ground to the total ground area [48]. FVC can be used to express the true vegetation coverage, greening level, and ecological environment quality of the study area (Jiang et al., 2017). In this study, we used NDVI, which is one of the most widely used

spectral vegetation indices in assessing vegetation greenness and its changes from local to global scales to approximate vegetation coverage [48]. The calculation of FVC based on NDVI follows:

$$\text{FVC} = \frac{\text{NDVI} - \text{NDVIsoil}}{\text{NDVIveg} - \text{NDVIsoil}} \tag{1}$$

where NDVIsoil is the NDVI value of bare soil, i.e., the NDVI value of areas without any vegetation coverage (equivalent to the minimum value of NDVI). NDVIveg is the NDVI value of pure vegetation pixels (equivalent to the maximum value of NDVI) [49,50]. Given the FVC values, we further classify different levels of vegetation containment, as shown in Table 1.

Table 1. Classification of vegetation coverage given FVC values in built-up areas of provincial capital cities.

Classification	FVC Interval	Features
Very Low FVC	$0 \leq \text{FVC} \leq 0.2$	No vegetation, soil, roads, lake, etc.
Low FVC	$0.2 < \text{FVC} \leq 0.4$	There is a small amount of vegetation, grass, etc.
Medium FVC	$0.4 < \text{FVC} \leq 0.6$	There is some vegetation, shrubs, etc.
High FVC	$0.6 < \text{FVC} \leq 0.8$	There is more vegetation, gardens. etc.
Very High FVC	$0.8 < \text{FVC} \leq 1.0$	There are a lot of vegetation, forests, etc.

Due to the influence of various factors, the value of NDVIsoil can differ spatially and temporally [51]. Given the differences in imaging time, vegetation type, and study areas, the values of NDVIveg can fluctuate as well. For the determination of NDVIsoil and NDVIveg, in order to prevent the interference of atmospheric radiations while removing noises, we refer to the national soil classification map and land-use map and field measurement data according to the actual vegetation coverage of the provincial capital. In addition, we refer to the national soil classification map and land-use map and field measurement data. We determine NDVIsoil as NDVI values between 2% and 5% and NDVIveg as NDVI values between 95% and 98%. The final FVC value range is normalized to a range of [0,1] [52].

2.3.2. Kernel Density Estimation

The kernel density estimation is based on the first law of geography that explores the spatial distribution of points and calculates the density of element points in the neighborhood [53,54]. In density analysis, points that fall into the search area have different weights. Points that are close to the search center are assigned larger weights [55]. The kernel density estimation follows:

$$f_{(s)} = \frac{1}{nh} \sum_{i=1}^{n} k\left(\frac{x - x_i}{h}\right) \tag{2}$$

where x_i represents the position coordinates of point i (i = 1, 2, ... , n); n is the number of element points; h is the search bandwidth of the kernel density calculation; the k function represents the spatial weight function [56–58]. The size of the output unit is the minimum width of the output range divided by 250. The search radius (i.e., bandwidth) is determined by the Silverman empirical rule [54] that can effectively avoid spatial outliers.

2.3.3. Spearman's Rank Correlation Coefficient

We calculate Spearman's rank correlation coefficient to quantitatively describe the relationship between the FVC of the built-up area of each provincial capital city and the regional GDP and the expansion speed of the built-up area (Tables S1–S3). Spearman's rank correlation coefficient test, a non-parametric test, measures the strength of the association between two variables [59]. The two elements are ranked in numerical order, and the rank

of the sample value of each element is used to replace the actual data [60]. Spearman's rank correlation coefficient can be calculated as:

$$R'_{xy} = 1 - \frac{6 \sum_{i=1}^{n} d_i^2}{n(n^2 - 1)} \tag{3}$$

where R'_{xy} is the Spearman rank correlation coefficient; n is the total number of sample squares; R_i and R_j are the ranks of element i and element j in the sample squares, respectively, $d_i = R_i - R_j$ [59].

We calculate the rank correlation coefficient between FVC and regional GDP in 2020 and find that their rank correlation is 0.7056. While the rank correlation coefficient between FVC and the expansion speed of built-up areas in 2020 is 0.7643. Both correlations are at the significance level of $\alpha = 0.01$, suggesting that FVC is strongly correlated with both regional GDP and the expansion rate of the built-up area of China's provincial capital cities in 2020.

3. Results

3.1. Differences in the Geographical Distribution of FVC

The study uses seven natural geographic regions divided by geographic location and climatic conditions. Compared with the four geographic regions divided by climate, the seven geographic regions comprehensively consider geographic location factors. In 1990, the average FVC of the built-up areas of capital cities in South China, East China, and Central China were 41.86%, 39.11%, and 36.35%. Much higher than the average FVC of 31.44%, 31.94%, 27.25%, and 27.53% in the built-up areas of capital cities in North China, South-west, North-west, and North-east China (Figure 3). Thirty years later, the average FVC in the built-up areas of capital cities in South China, East China, Central China reached 43.73%, 45.43%, 41.83%, while the average FVC in North China, South-west, North-west, and North-east China reached 44.10%, 39.00%, 35.21%, 41.99%.
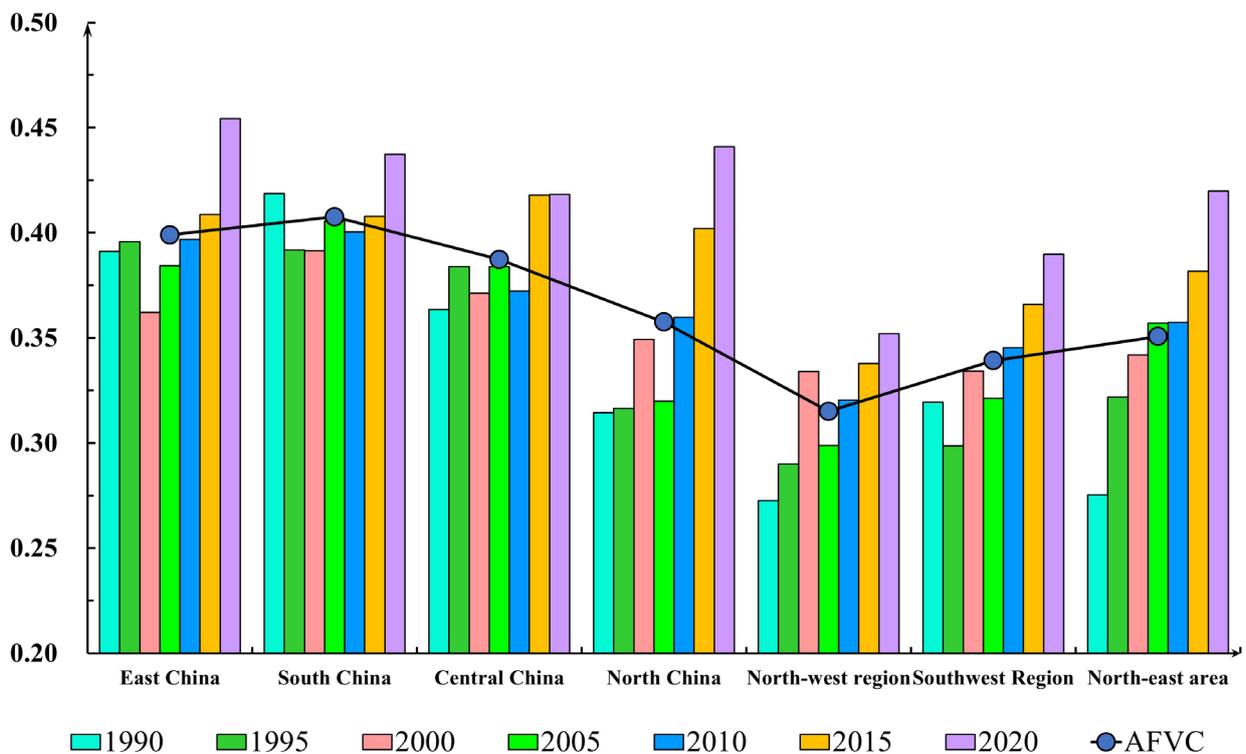

**Figure 3.** FVC changes in built-up areas of capital cities in seven geographic regions from 1990 to 2020.

From 1990 to 2020, the FVC in the built-up areas of the capital cities of the seven geographic regions has shown an upward trend, with the FVC in the capital cities in North China having the highest increase by 12.66%. The above results show that the natural geographic environment is one of the main reasons for the difference in urban vegetation coverage, but with the continuous development of urbanization, the image of vegetation coverage has weakened. However, it still presents the spatial distribution characteristics of low vegetation coverage in the built-up areas of capital cities in the South-west and North-west China and high vegetation coverage in the built-up areas of capital cities in South China, East China, and North China.

3.2. Changes in the Spatial Pattern of FVC

Taking several cities as examples (Figure 4), we can observe that in 1990, areas with low-FVC were mainly concentrated in the center of urban built-up areas, showing a contiguous distribution pattern, occupying a considerable part of the total built-up area. The areas with high-FVC are mainly concentrated on the edge of the urban built-up area, presenting a patchy distribution pattern, while the proportion of the area of high-FVC in the total area of the built-up area is considerably low. This shows that in the early stage of urban construction, urban built-up areas have very low-FVC, indicating that urban greenness planning is a disordered state and the distribution is unreasonable [18]. With the continuous advancement of urbanization, by 2020, low-FVC areas and high-FVC areas in the built-up areas of provincial capital cities have evolved from a centralized distribution pattern to a uniform distribution pattern, showing notable vegetation patches [61]. Areas with high-FVC are no longer confined to the urban fringe areas but more evenly distributed within urban built-up areas, with low-FVC areas scattered in between. Comparing with the FVC classification maps of other provincial capitals, we notice that such phenomena exist in 31 provincial capitals, demonstrating the great universality of the above conclusion that summarizes the changing spatial patterns of vegetation coverage in urban built-up areas.

Based on the analysis of the kernel density of the vegetation in the built-up areas of Beijing, Guangzhou, and Zhengzhou from 1990 to 2020, we noticed that the central vegetation in the built-up areas of provincial capital cities had increased year by year. The "hollowing" phenomenon of the vegetation in the built-up areas has gradually disappeared. In addition, a wider "Urban Green Belt" has been formed at the periphery of urban built-up areas with improved connectivity of areas with high-FVC (Figure 5).

This shows that in the middle and late stages of urban construction, urban public green spaces, residential green spaces, traffic green spaces, and scenic green spaces have been well organized [62], evidenced by their evenly distributed patterns within the urban built-up areas. Urban green space has gradually changed from a relatively concentrated "green heart" distribution pattern to a relatively scattered "green pulse" distribution pattern (Figure 6) [63]. Such a layout of green space in urban built-up areas tends to be reasonable and can meet the needs of urban residents.
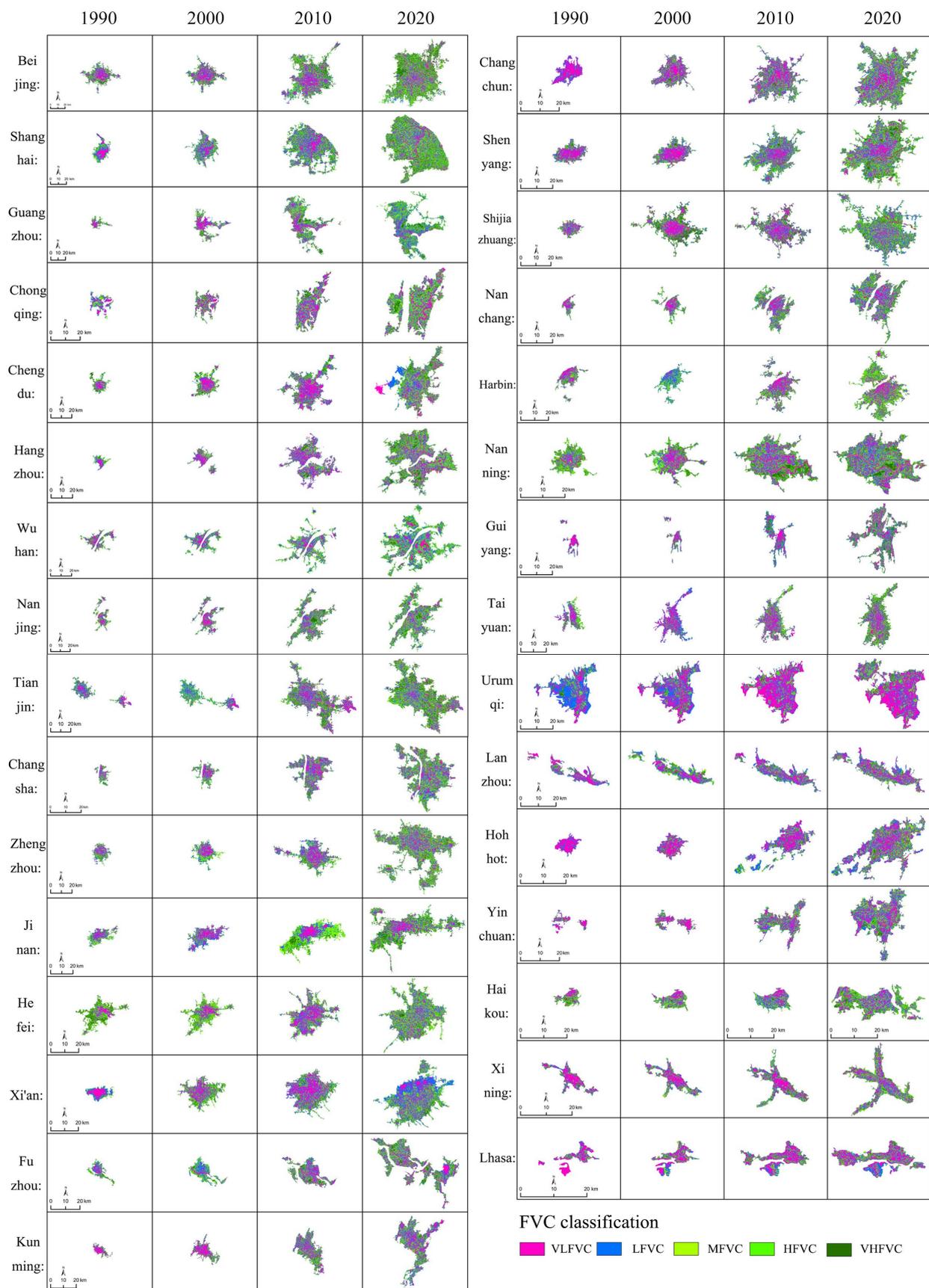
Figure 4. FVC hierarchical chart in built-up areas of provincial capital cities from 1990 to 2020. (VLFVC: very low FVC; LFVC: low FVC; MFVC: medium FVC; HFVC: high FVC; VFVC: very High FVC).
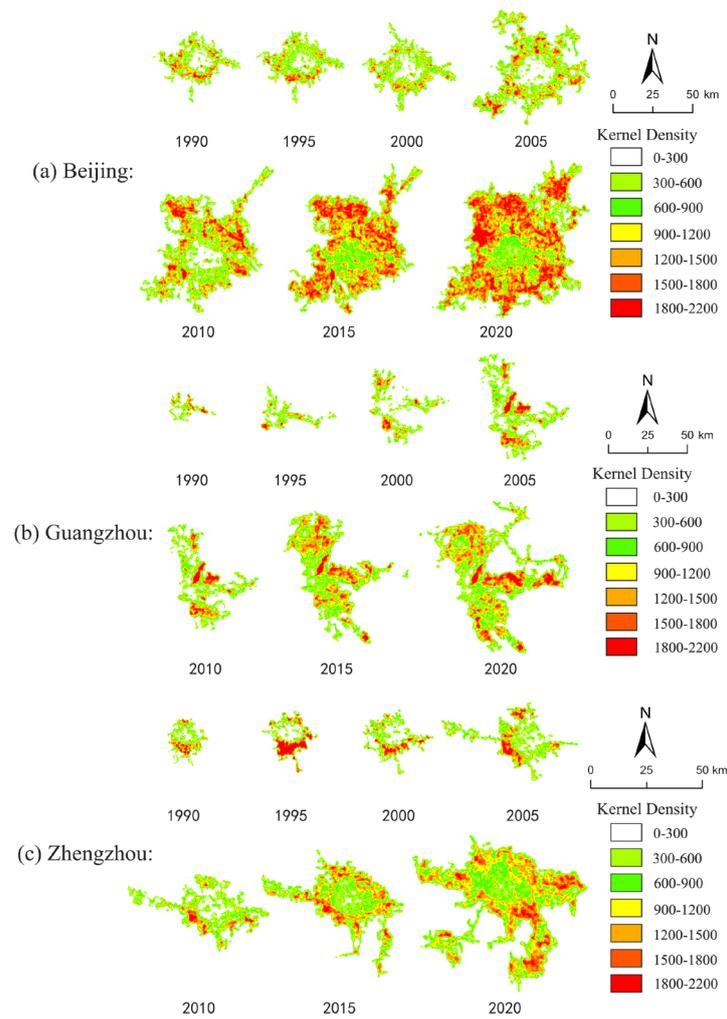
Figure 5. Distribution map of kernel density of vegetation in Beijing's (**a**), Guangzhou's (**b**), Zhengzhou's (**c**), built-up area from 1990 to 2020.

(a) "Green Heart" distribution model   **(b) "Green Vein" distribution model**
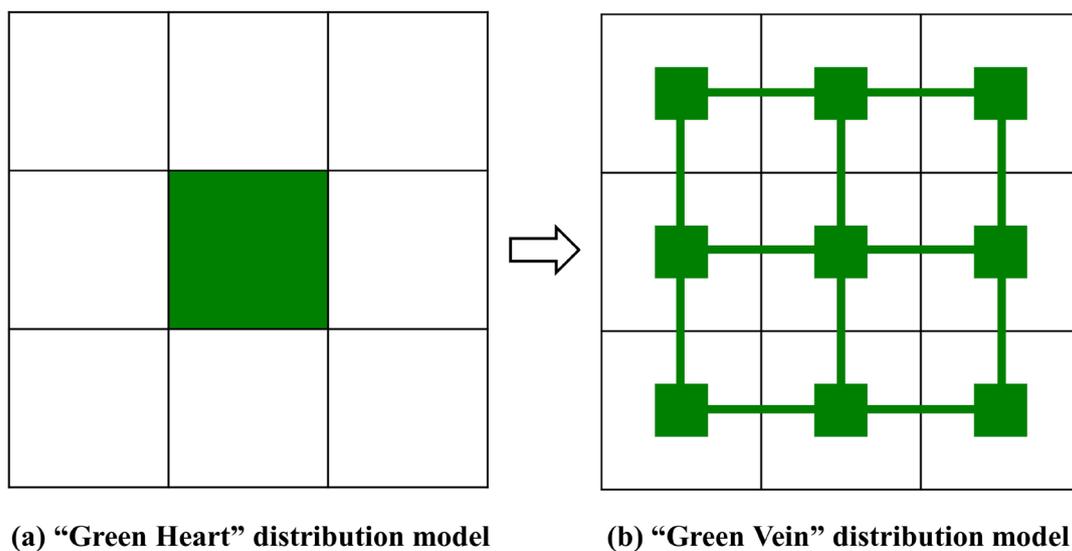
Figure 6. The evolution model of green space in urban built-up areas.

3.3. The Overall Trend of FVC in the Past Three Decades

Figure 7 shows the change of the overall average FVC in the built-up areas of provincial capital cities in mainland China from 1990 to 2020. It can be clearly seen that the overall average FVC in the built-up areas of 31 provincial capital cities has shown an upward trend in the past 30 years. In 1990, the overall FVC in the built-up areas of provincial capital cities was 33.59%. By 2020, the overall average FVC in the built-up areas of provincial capital cities reached 41.56%, an increase of 7.97% compared to 1990. The above results suggest that in the past 30 years, the vegetation coverage in urban built-up areas has considerably increased. The urban ecological environments have undergone a notable transition, leading to the improved sustainable development of urban ecology.
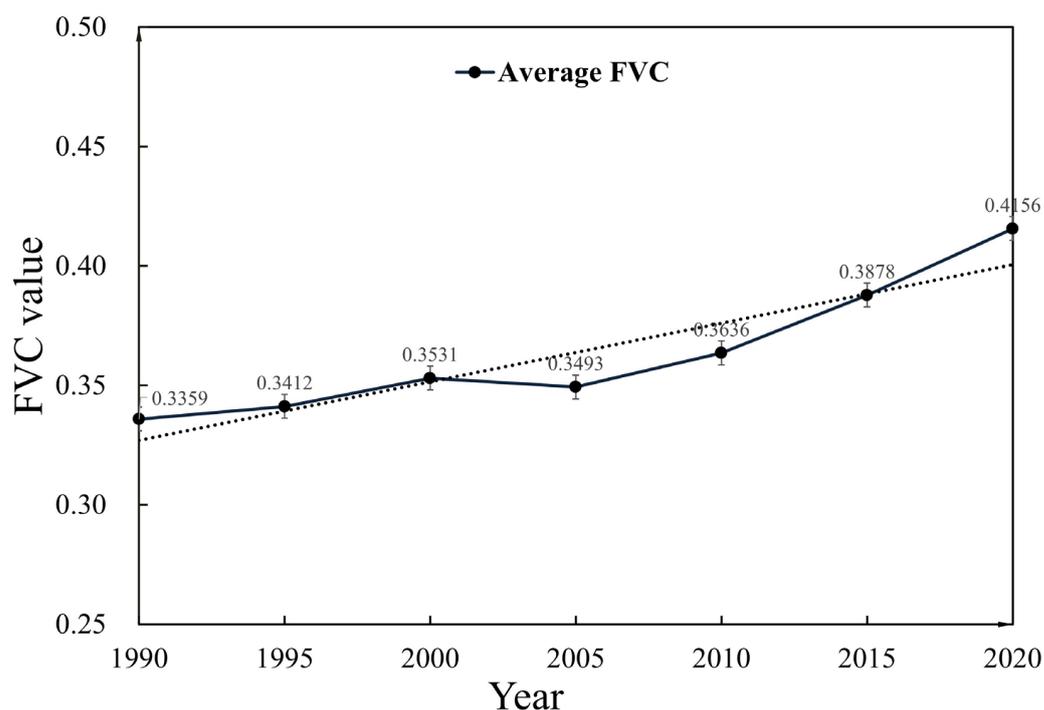

Figure 7. Changes in average FVC of provincial capital cities from 1990 to 2020.

As shown in Table S1, from 1990 to 2020, 28 cities (out of 31) have a positive change in the average FVC in built-up areas; 22 cities have an average FVC growth rate of more than 5% in the built-up areas of provincial capitals, accounting for 70.97% of the total number of cities. In addition, 12 cities have a growth rate of more than 10%. The FVC of the built-up area of Beijing increased from 37.62% to 50.30%. The 50.30% FVC of Beijing ranks the first among all provincial capital cities in 2020; the FVC of the built-up area of Tianjin is 48.74% in 2020, ranking second; the FVC in the built-up area of Shanghai increased from 33.01% to 47.96% from 1990 to 2020. Its FVC in 2020 ranks third. Notably, the FVC in Hohhot City increased from 15.54% to 33.94%, with a change rate of 18.4%; the FVC in the built-up area of Changchun City increased from 17.71% in 1990 to 38.61%, with a change rate of more than 20%. Cities with negative changes in FVC include Chengdu (−2.43%), Fuzhou (−0.77%), and Haikou (−0.71%). In general, the FVC reduction values in these three cities are relatively small, within the normal fluctuation range. Our results coincide with existing efforts that also documented the increase of FVC in built-up areas of provincial capital cities in mainland China [15,32–35].

In this study, pixels with $0 \leq FVC \leq 0.4$ are deemed to have no vegetation coverage. The vegetation coverage ratio denotes the ratio of the vegetation area to the total area of the built-up area. In this study, we use statistical data to calculate the yearly vegetation coverage rate in the built-up area of the provincial capital city, as shown in Tables S2 and S3. The results show that between 1990 and 2020, the vegetation coverage rate of built-up areas

in most provincial capital cities has increased in a significant manner, with only several provincial capital cities having slightly decreased vegetation coverage rate in the built-up areas. The vegetation coverage in the built-up areas of provincial capital cities has been significantly improved during the investigated period. As shown in Figure 8, in 1990, there were only nine cities with medium, high, and very high FVC areas, accounting for more than 40%. In 2020, this number increased to 27 cities. As of 2020, 25 cities have increased the proportion of medium, high, and very high FVC in urban built-up areas, accounting for 87.10% of the total number of cities. There is a total of 22 cities with the proportion of medium, high, and very high FVC increased by more than 10%. Beijing, Shanghai, Tianjin, Shenyang, Changchun, Guiyang, Hohhot, among others, have increased the proportion of medium, high, and very high FVC areas by more than 20%. Despite that, our results suggest, in the past 30 years, the medium, high, and very high FVC areas in the built-up areas of provincial capital cities have increased significantly, and areas with high and very high FVC in the total urban area are still low, indicating the potential of further improvement to urban ecological green space.
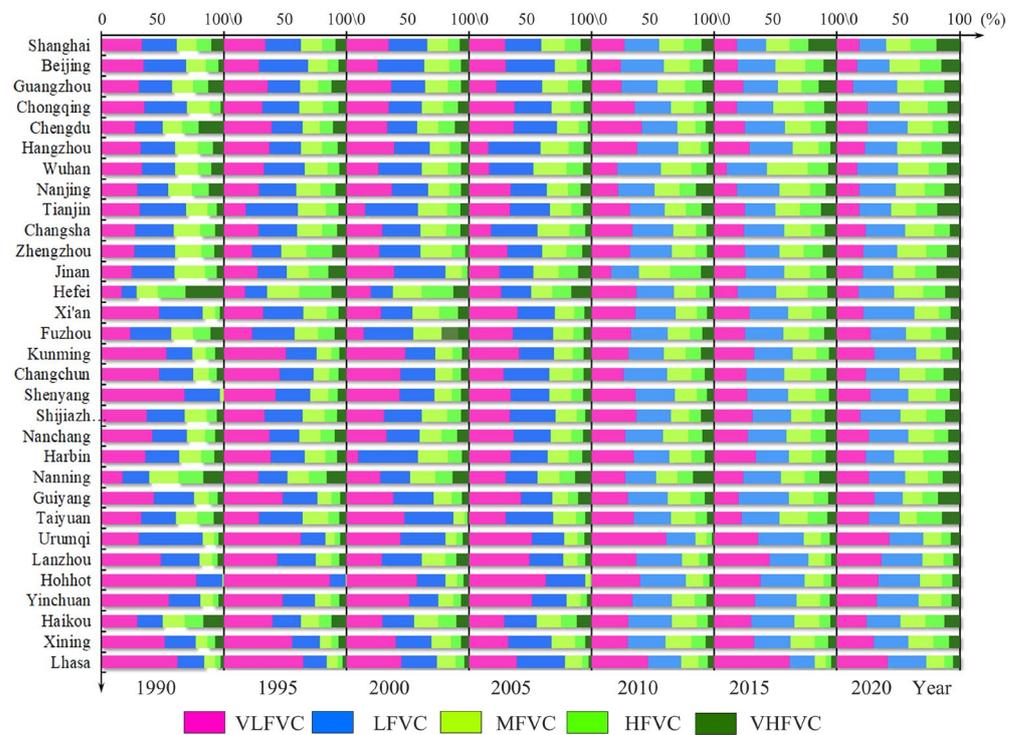
Figure 8. Percentage accumulation FVC of different grades in provincial capital cities from 1990 to 2020.

3.4. The FVC Temporal Dynamic Curve

Figure 9 shows the temporal dynamics of the FVC in the built-up areas of provincial capital cities in mainland China from 1990 to 2020. A positive value indicates that the vegetation coverage has increased compared with the previous stage, and a negative value indicates that the vegetation coverage has decreased compared with the previous stage. In general, the FVC change curves in the urban built-up areas are in complex patterns, with strong dynamics, continuous undulating, and oscillating rising (Figure 9a). In addition, we notice that the amplitude of the oscillation is gradually weakening. In 1990, there were only six provincial capital cities with FVC between 40%–50% in built-up areas. By 2020, this number increased to 21, accounting for about 67.74% of the total number of provincial capital cities. The FVC in the built-up areas of most provincial capital cities showed an increasing trend, with several exceptions. Numerous studies have shown that in the process of urbanization, the FVC in the built-up areas of most provincial capital cities

is expected to increase but within a limited range [15,32–35]. The FVC tends to keep in the range of 40%–50%, an optimal range that balances the development and urban ecological environment quality (Figure 9b–d).
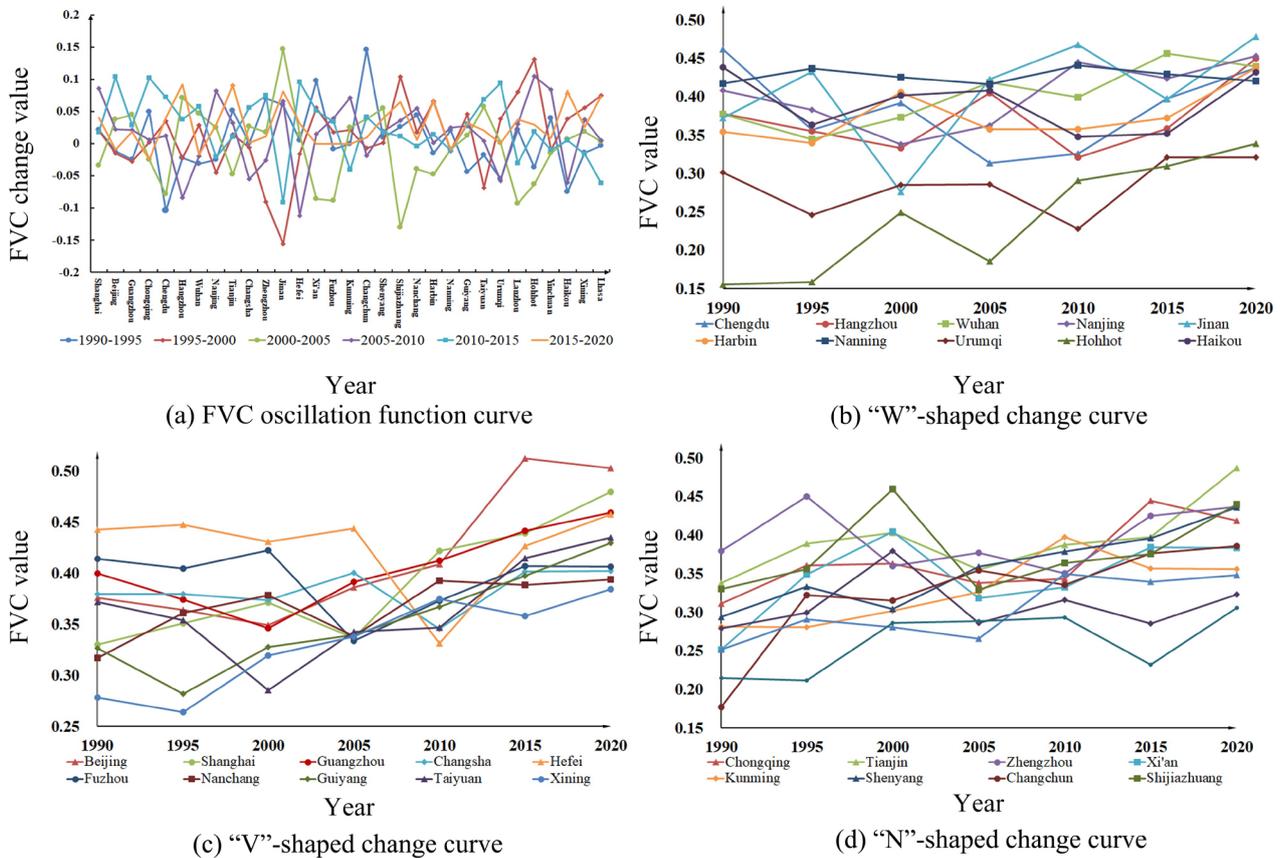

(a) FVC oscillation function curve

(b) "W"-shaped change curve

(c) "V"-shaped change curve

(d) "N"-shaped change curve

Figure 9. FVC changing curves of built-up areas of provincial capital cities from 1990 to 2020.

At the city-level, the temporal dynamics of the FVC in urban built-up areas can be mainly expressed as "W" type (decrease-increase-decrease-increase) curve (Figure 9b), a "V" type (decrease-increase) curve (Figure 9c), and "N" type (increase-decrease-increase) (Figure 9d). Cities represented by the "W"-shaped change curve include Chengdu, Hangzhou, Wuhan, Nanjing, Jinan, among others. In those cities, the FVC of built-up areas of provincial capital cities first decreased from 1990 to 1995, increased from 1995 to 2005, decreased again from 2005 to 2010, and then increased from 2010 to 2020. The cities represented by the "V"-shaped changing curves include Beijing, Shanghai, Guangzhou, Changsha, Hefei, among others. For those cities, FVC fluctuated during 1990–1995, decreased from 2000 to 2010, and began to increase after 2010. Cities represented by the "N"-shaped changing curves include Chongqing, Tianjin, Zhengzhou, Xi'an, Kunming, among others. In those cities, FVC experienced a decreasing trend from 1990 to 2000, and an increasing trend occurred from 2005 to 2020.

4. Discussion

4.1. Influencing Factors of Spatial Disparity in Vegetation Coverage

Numerous factors can lead to the disparity in FVC of the built-up areas of provincial capital cities. Those factors include the natural geographic environment, climate change, economic development level, built-up area expansion, ecological green space construction, and land type conversion [39,64,65]. Among them, the economic development level of provincial capitals can be represented by the regional GDP. As shown in Table S1, for the top ten provincial capital cities in terms of regional GDP in 2020, the FVC of built-up areas of them are all greater than 40%. In addition, the rank correlation coefficient of FVC

in provincial capital city built-up areas and regional GDP is 0.7056, indicating that the vegetation coverage of the provincial capital city's built-up area has a substantial positive link with the level of economic development, which is consistent with previous studies [37]. While the rank correlation coefficient between FVC and the expansion speed of built-up areas in 2020 is 0.7643. This further illustrates that the expansion of built-up areas has led to an increase in urban vegetation coverage, but this increase mainly comes from the periphery of the built-up area, because a large amount of undeveloped green space is still reserved on the periphery of the built-up area.

At the same time, the vegetation coverage of cities such as Guiyang, Nanning, Haikou, etc., is still greater than 40% despite their lagging regional GDP ranking in 2020. This shows that the natural geographical environment is one of the main factors that affect FVC in the built-up areas of provincial capitals, and due to the influence of the natural geographical environment, provincial capital cities of mainland China present the spatial distribution characteristics of low vegetation coverage in the built-up areas of capital cities in southwest, northwest regions, and high vegetation coverage in the built-up areas of capital cities in South China, East China, and North China. For other cities, such as Harbin and Shenyang, where the natural geographical environment and economic development level are relatively weak, their FVC of the built-up area is also greater than 40%, presumably due to their long history of city construction, the longtime urban development, and the complete urbanization process. On the contrary, Kunming, known as the "Spring City" as well as a famous scenic tourist city in China, has superior natural geographic environments with a high level of economic development. However, the FVC of Kunming's built-up area in 2020 is only 35.64%. The example of Kunming shows that the FVC in urban built-up areas can be subject to policies and the greening policies issued by the government can motivate or dampen the restoration of vegetation and the construction of ecological green spaces in urban built-up areas.

4.2. Reasons for the Evolution of the Spatial Pattern of Vegetation Coverage

The reasons for the evolution of the FVC spatial pattern of provincial capitals are multi-faceted. On the one hand, due to the continuous outward expansion of cities, urban built-up areas have greatly increased [66], while the edge of the built-up area has not been developed in a timely and effective manner, e.g., farmland, villages, and woodland. In this process, FVC is expected to follow an increasing pattern. With the progress of continuous development, land cover types at the edge of the built-up area begin to change, with a large number of urban green spaces transforming into non-green space, such as residential, commercial and business facilities, industrial, road, street, and transportation, resulting in a decrease in FVC in the built-up area. The reason why our conclusions differ from previous ones is that we consider both urban expansion and FVC changes [35].

Furthermore, in the early stage of urban construction, the low vegetation coverage area in the center of the built-up area tends to present a concentrated flaky distribution. The reason is that the layout of the built-up area in urban centers is relatively concentrated. With the improvement of socio-economic levels and the expectation of boosted living conditions, urban residents start to pay more attention to the quality of the urban ecological environment, pushing local governments to increase the construction of urban green space. Thus, the overall greening levels of urban built-up areas begin to improve in the later developing stage, with a more reasonable distribution of urban green spaces.

4.3. Causes of the Evolution Model of FVC

The main reasons for the "oscillating function" change pattern of vegetation coverage in built-up areas of provincial capital cities are built-up area expansion, ecological green space construction, land type conversion, etc. The expansion of built-up areas and the construction of ecological green spaces will lead to an increase in FVC, while the transformation of land types will lead to a decrease in FVC. The decrease or increase of the average FVC in the built-up area of the provincial capital city in that year depends on the positive factor and

the negative factor among the three influencing factors, of which the type of factor plays a leading role. This is also the reason why the evolution of urban vegetation coverage presents a dynamic, continuous, oscillating, and rising "oscillating function" change pattern.

However, because cities must retain a large amount of residential, public, commercial, industrial, road, etc., the increase in vegetation coverage is not endless, but there is a certain limit. With the implementation of the new urbanization development concept centered on people and the sustainable development of ecologically civilized cities, eventually, the vegetation coverage change curve in the built-up areas of provincial capital cities will tend to stabilize. It can be speculated that in the later stage of urban construction, the urban vegetation coverage will tend to a range between 40–50%. It is the optimal interval that comprehensively considers economic construction, social development, and ecological environment quality.

5. Conclusions

In this study, we use urban boundary mapping of the artificial impervious surface from GAIA, extract remote sensing images of built-up areas of provincial capital cities, calculate the NDVI, estimate the FVC, and evaluate the FVC spatiotemporal changing dynamics of the built-up areas in 31 provincial capitals in the mainland China. We further use Spearman's rank correlation coefficient to identify the influencing factors of vegetation coverage in urban built-up areas and kernel density estimation to explore the spatial distribution of vegetation coverage. Our results suggest that (1) From 1990 to 2020, the average FVC of the built-up areas of 31 provincial capital cities increased by 7.97%, and the proportion of medium, high, and very high vegetation coverage areas increased by 12.45%. In addition, we observe that the urban green space has gradually changed from the "green heart" distribution model to the "green vein" distribution model. (2) Due to the influence of various factors, such as natural geographic environment, economic development level, built-up area expansion, land type transformation, afforestation of greening policy, etc., provincial capital cities present great disparity in FVC changing curves, which can be mainly divided into the "W" type (decrease-increase-decrease-increase), the "V" type (decrease-increase), and the "N" type (increase-decrease-increase); (3) The FVC of the built-up area of provincial capital cities is significantly correlated with the regional GDP and the expansion speed of the built-up area. The expansion of the built-up area and the construction of ecological green space are positively correlated with the increase of FVC. The initial value of FVC in built-up areas and the level of economic development drive the disparity in FVC changing patterns. The FVC curves of the built-up area of the provincial capital city present an "oscillation function" changing pattern, with weakening amplitudes. The FVC eventually falls in the range of 40%–50%, which is considered an optimal value that balances the economic/social development and ecological environment quality. The study is expected to provide scientific references of an important theoretical basis for urban ecological construction and practical support for promoting the harmonious development of urban residents and urban environments in China.

Author Contributions: Conceptualization, J.C. and Z.Y.; methodology, M.L.; writing—review and editing, J.C. and X.H. All authors have read and agreed to the published version of the manuscript.

Data Availability Statement: The datasets generated during and analyzed in this study are publicly available. All data and scripts are available from the corresponding author on request.

Conflicts of Interest: The authors declare that they have no known competing financial interests or personal relationships that could have appeared to influence the work reported in this paper.

References

1. Yu, B. Ecological Effects of New-Type Urbanization in China. *Renew. Sustain. Energy Rev.* **2021**, *135*, 110239. [CrossRef]
2. Chen, J.; Shao, Z.; Huang, X.; Zhuang, Q.; Dang, C.; Cai, B.; Zheng, X.; Ding, Q. Assessing the Impact of Drought-Land Cover Change on Global Vegetation Greenness and Productivity. *Sci. Total Environ.* **2022**, *852*, 158499. [CrossRef]
3. Zhou, D.; Xiao, J.; Bonafoni, S.; Berger, C.; Deilami, K.; Zhou, Y.; Frolking, S.; Yao, R.; Qiao, Z.; Sobrino, J.A. Satellite Remote Sensing of Surface Urban Heat Islands: Progress, Challenges, and Perspectives. *Remote Sens.* **2019**, *11*, 48. [CrossRef]
4. Shao, Z.; Ding, L.; Li, D.; Altan, O.; Huq, E. Exploring the Relationship between Urbanization and Ecological Environment Using Remote Sensing Images and Statistical Data: A Case Study in the Yangtze River Delta, China. *Sustainability* **2020**, *12*, 5620. [CrossRef]
5. Lee, A.C.K.; Maheswaran, R. The Health Benefits of Urban Green Spaces: A Review of the Evidence. *J. Public Health* **2011**, *33*, 212–222. [CrossRef]
6. Estoque, R.C.; Murayama, Y.; Myint, S.W. Effects of Landscape Composition and Pattern on Land Surface Temperature: An Urban Heat Island Study in the Megacities of Southeast Asia. *Sci. Total Environ.* **2017**, *577*, 349–359. [CrossRef]
7. Nesbitt, L.; Meitner, M.J.; Girling, C.; Sheppard, S.R.J.; Lu, Y. Who Has Access to Urban Vegetation? A Spatial Analysis of Distributional Green Equity in 10 US Cities. *Landsc. Urban Plan.* **2019**, *181*, 51–79. [CrossRef]
8. Zhang, J.; Yu, Z.; Cheng, Y.; Chen, C.; Wan, Y.; Zhao, B.; Vejre, H. Evaluating the Disparities in Urban Green Space Provision in Communities with Diverse Built Environments: The Case of a Rapidly Urbanizing Chinese City. *Build. Environ.* **2020**, *183*, 107170. [CrossRef]
9. Markevych, I.; Schoierer, J.; Hartig, T.; Chudnovsky, A.; Hystad, P.; Dzhambov, A.M.; de Vries, S.; Triguero-Mas, M.; Brauer, M.; Nieuwenhuijsen, M.J.; et al. Exploring Pathways Linking Greenspace to Health: Theoretical and Methodological Guidance. *Environ. Res.* **2017**, *158*, 301–317. [CrossRef]
10. Zhang, Y.; Shao, Z. Assessing of Urban Vegetation Biomass in Combination with LiDAR and High-Resolution Remote Sensing Images. *Int. J. Remote Sens.* **2021**, *42*, 964–985. [CrossRef]
11. Zhao, W.; Li, A.; Huang, Q.; Gao, Y.; Li, F.; Zhang, L. An Improved Method for Assessing Vegetation Cooling Service in Regulating Thermal Environment: A Case Study in Xiamen, China. *Ecol. Indic.* **2019**, *98*, 531–542. [CrossRef]
12. Bowler, D.E.; Buyung-Ali, L.; Knight, T.M.; Pullin, A.S. Urban Greening to Cool Towns and Cities: A Systematic Review of the Empirical Evidence. *Landsc. Urban Plan.* **2010**, *97*, 147–155. [CrossRef]
13. Amani-Beni, M.; Zhang, B.; Xie, G.-d.; Xu, J. Impact of Urban Park's Tree, Grass and Waterbody on Microclimate in Hot Summer Days: A Case Study of Olympic Park in Beijing, China. *Urban For. Urban Green.* **2018**, *32*, 1–6. [CrossRef]
14. Zhuang, Q.; Shao, Z.; Gong, J.; Li, D.; Huang, X.; Zhang, Y.; Xu, X.; Dang, C.; Chen, J.; Altan, O.; et al. Modeling Carbon Storage in Urban Vegetation: Progress, Challenges, and Opportunities. *Int. J. Appl. Earth Obs. Geoinf.* **2022**, *114*, 103058. [CrossRef]
15. Piao, S.; Wang, X.; Park, T.; Chen, C.; Lian, X.; He, Y.; Bjerke, J.W.; Chen, A.; Ciais, P.; Tømmervik, H.; et al. Characteristics, Drivers and Feedbacks of Global Greening. *Nat. Rev. Earth Environ.* **2020**, *1*, 14–27. [CrossRef]
16. Davies, Z.G.; Edmondson, J.L.; Heinemeyer, A.; Leake, J.R.; Gaston, K.J. Mapping an Urban Ecosystem Service: Quantifying above-Ground Carbon Storage at a City-Wide Scale. *J. Appl. Ecol.* **2011**, *48*, 1125–1134. [CrossRef]
17. Fischer, L.K.; Honold, J.; Botzat, A.; Brinkmeyer, D.; Cvejić, R.; Delshammar, T.; Elands, B.; Haase, D.; Kabisch, N.; Karle, S.J.; et al. Recreational Ecosystem Services in European Cities: Sociocultural and Geographical Contexts Matter for Park Use. *Ecosyst. Serv.* **2018**, *31*, 455–467. [CrossRef]
18. Zhang, J.; Yu, Z.; Zhao, B.; Sun, R.; Vejre, H. Links between Green Space and Public Health: A Bibliometric Review of Global Research Trends and Future Prospects from 1901 to 2019. *Environ. Res. Lett.* **2020**, *15*, 063001. [CrossRef]
19. Santamouris, M.; Ban-Weiss, G.; Osmond, P.; Paolini, R.; Synnefa, A.; Cartalis, C.; Muscio, A.; Zinzi, M.; Morakinyo, T.E.; Ng, E.; et al. Progress in Urban Greenery Mitigation Science—Assessment Methodologies Advanced Technologies and Impact on Cities. *J. Civ. Eng. Manag.* **2018**, *24*, 638–671. [CrossRef]
20. Nowak, D.J.; Hirabayashi, S.; Doyle, M.; McGovern, M.; Pasher, J. Air Pollution Removal by Urban Forests in Canada and Its Effect on Air Quality and Human Health. *Urban For. Urban Green.* **2018**, *29*, 40–48. [CrossRef]
21. Sarkar, C.; Webster, C.; Gallacher, J. Residential Greenness and Prevalence of Major Depressive Disorders: A Cross-Sectional, Observational, Associational Study of 94 879 Adult UK Biobank Participants. *Lancet Planet. Health* **2018**, *2*, e162–e173. [CrossRef]
22. Bratman, G.N.; Anderson, C.B.; Berman, M.G.; Cochran, B.; De Vries, S.; Flanders, J.; Folke, C.; Frumkin, H.; Gross, J.J.; Hartig, T.; et al. Nature and Mental Health: An Ecosystem Service Perspective. *Sci. Adv.* **2019**, *5*, eaax0903. [CrossRef]
23. Cheng, Y.; Zhang, J.; Wei, W.; Zhao, B. Effects of Urban Parks on Residents' Expressed Happiness before and during the COVID-19 Pandemic. *Landsc. Urban Plan.* **2021**, *212*, 104118. [CrossRef]
24. Wu, L.; Kim, S.K. Does Socioeconomic Development Lead to More Equal Distribution of Green Space? Evidence from Chinese Cities. *Sci. Total Environ.* **2021**, *757*, 143780. [CrossRef]
25. Chen, C.; Park, T.; Wang, X.; Piao, S.; Xu, B.; Chaturvedi, R.K.; Fuchs, R.; Brovkin, V.; Ciais, P.; Fensholt, R.; et al. China and India Lead in Greening of the World through Land-Use Management. *Nat. Sustain.* **2019**, *2*, 122–129. [CrossRef]
26. Gong, P.; Wang, J.; Yu, L.; Zhao, Y.; Zhao, Y.; Liang, L.; Niu, Z.; Huang, X.; Fu, H.; Liu, S.; et al. Finer Resolution Observation and Monitoring of Global Land Cover: First Mapping Results with Landsat TM and ETM+ Data. *Int. J. Remote Sens.* **2013**, *34*, 2607–2654. [CrossRef]

27. Li, J.; Peng, S.; Li, Z. Detecting and Attributing Vegetation Changes on China's Loess Plateau. *Agric. For. Meteorol.* **2017**, *247*, 260–270. [CrossRef]

28. Zheng, K.; Wei, J.Z.; Pei, J.Y.; Cheng, H.; Zhang, X.L.; Huang, F.Q.; Li, F.M.; Ye, J.S. Impacts of Climate Change and Human Activities on Grassland Vegetation Variation in the Chinese Loess Plateau. *Sci. Total Environ.* **2019**, *660*, 236–244. [CrossRef]

29. Chen, B.; Nie, Z.; Chen, Z.; Xu, B. Quantitative Estimation of 21st-Century Urban Greenspace Changes in Chinese Populous Cities. *Sci. Total Environ.* **2017**, *609*, 956–965. [CrossRef]

30. Li, R.; Zheng, S.; Duan, C.; Wang, L.; Zhang, C. Land Cover Classification from Remote Sensing Images Based on Multi-Scale Fully Convolutional Network. *Geo-Spat. Inf. Sci.* **2022**, *25*, 278–294. [CrossRef]

31. Wu, H.; Gui, Z.; Yang, Z. Geospatial Big Data for Urban Planning and Urban Management. *Geo-Spat. Inf. Sci.* **2020**, *23*, 273–274. [CrossRef]

32. Piao, S.; Yin, G.; Tan, J.; Cheng, L.; Huang, M.; Li, Y.; Liu, R.; Mao, J.; Myneni, R.B.; Peng, S.; et al. Detection and Attribution of Vegetation Greening Trend in China over the Last 30 Years. *Glob. Chang. Biol.* **2015**, *21*, 1601–1609. [CrossRef]

33. Feng, D.; Bao, W.; Yang, Y.; Fu, M. How Do Government Policies Promote Greening? Evidence from China. *Land Use Policy* **2021**, *104*, 105389. [CrossRef]

34. Luo, Y.; Sun, W.; Yang, K.; Zhao, L. China Urbanization Process Induced Vegetation Degradation and Improvement in Recent 20 Years. *Cities* **2021**, *114*, 103207. [CrossRef]

35. Mu, B.; Zhao, X.; Wu, D.; Wang, X.; Zhao, J.; Wang, H.; Zhou, Q.; Du, X.; Liu, N. Vegetation Cover Change and Its Attribution in China from 2001 to 2018. *Remote Sens.* **2021**, *13*, 496. [CrossRef]

36. Zhuang, Q.; Wu, S.; Feng, X.; Niu, Y. Analysis and Prediction of Vegetation Dynamics under the Background of Climate Change in Xinjiang, China. *PeerJ* **2020**, *8*, e8282. [CrossRef]

37. Hu, M.; Xia, B. A Significant Increase in the Normalized Difference Vegetation Index during the Rapid Economic Development in the Pearl River Delta of China. *Land Degrad. Dev.* **2019**, *30*, 359–370. [CrossRef]

38. Zhou, Q.; Zhao, X.; Wu, D.; Tang, R.; Du, X.; Wang, H.; Zhao, J.; Xu, P.; Peng, Y. Impact of Urbanization and Climate on Vegetation Coverage in the Beijing-Tianjin-Hebei Region of China. *Remote Sens.* **2019**, *11*, 2452. [CrossRef]

39. Jiang, M.; Tian, S.; Zheng, Z.; Zhan, Q.; He, Y. Human Activity Influences on Vegetation Cover Changes in Beijing, China, from 2000 to 2015. *Remote Sens.* **2017**, *9*, 271. [CrossRef]

40. Gui, X.; Wang, L.; Yao, R.; Yu, D.; Li, C. Investigating the Urbanization Process and Its Impact on Vegetation Change and Urban Heat Island in Wuhan, China. *Environ. Sci. Pollut. Res.* **2019**, *26*, 30808–30825. [CrossRef]

41. Shao, Z.; Wu, W.; Li, D. Spatio-Temporal-Spectral Observation Model for Urban Remote Sensing. *Geo-Spat. Inf. Sci.* **2021**, *24*, 372–386. [CrossRef]

42. Zhu, Z.; Piao, S.; Myneni, R.B.; Huang, M.; Zeng, Z.; Canadell, J.G.; Ciais, P.; Sitch, S.; Friedlingstein, P.; Arneth, A.; et al. Greening of the Earth and Its Drivers. *Nat. Clim. Change* **2016**, *6*, 791–795. [CrossRef]

43. Farhadi, H.; Esmaeily, A.; Najafzadeh, M. Flood Monitoring by Integration of Remote Sensing Technique and Multi-Criteria Decision Making Method. *Comput. Geosci.* **2022**, *160*, 105045. [CrossRef]

44. Farhadi, H.; Mokhtarzade, M.; Ebadi, H.; Beirami, B.A. Rapid and Automatic Burned Area Detection Using Sentinel-2 Time-Series Images in Google Earth Engine Cloud Platform: A Case Study over the Andika and Behbahan Regions, Iran. *Environ. Monit. Assess.* **2022**, *194*, 369. [CrossRef]

45. Farhadi, H.; Mohammad, N. Flood Risk Mapping by Remote Sensing Data and Random. *Water* **2021**, *13*, 3115. [CrossRef]

46. Huang, X.; Liu, A.; Li, J. Mapping and Analyzing the Local Climate Zones in China's 32 Major Cities Using Landsat Imagery Based on a Novel Convolutional Neural Network. *Geo-Spat. Inf. Sci.* **2021**, *24*, 528–557. [CrossRef]

47. Li, X.; Gong, P.; Zhou, Y.; Wang, J.; Bai, Y.; Chen, B.; Hu, T.; Xiao, Y.; Xu, B.; Yang, J.; et al. Mapping Global Urban Boundaries from the Global Artificial Impervious Area (GAIA) Data. *Environ. Res. Lett.* **2020**, *15*, 094044. [CrossRef]

48. Gao, L.; Wang, X.; Johnson, B.A.; Tian, Q.; Wang, Y.; Verrelst, J.; Mu, X.; Gu, X. Remote Sensing Algorithms for Estimation of Fractional Vegetation Cover Using Pure Vegetation Index Values: A Review. *ISPRS J. Photogramm. Remote Sens.* **2020**, *159*, 364–377. [CrossRef]

49. Carlson, T.N.; Ripley, D.A. On the Relation between NDVI, Fractional Vegetation Cover, and Leaf Area Index. *Remote Sens. Environ.* **1997**, *62*, 241–252. [CrossRef]

50. Ge, J.; Meng, B.; Liang, T.; Feng, Q.; Gao, J.; Yang, S.; Huang, X.; Xie, H. Modeling Alpine Grassland Cover Based on MODIS Data and Support Vector Machine Regression in the Headwater Region of the Huanghe River, China. *Remote Sens. Environ.* **2018**, *218*, 162–173. [CrossRef]

51. Rundquist, B.C. The Influence of Canopy Green Vegetation Fraction on Spectral Measurements over Native Tallgrass Prairie. *Remote Sens. Environ.* **2002**, *81*, 129–135. [CrossRef]

52. Zeng, X.; Dickinson, R.E.; Walker, A.; Shaikh, M.; Defries, R.S.; Qi, J. Derivation and Evaluation of Global 1-Km Fractional Vegetation Cover Data for Land Modeling. *J. Appl. Meteorol.* **2000**, *39*, 826–839. [CrossRef]

53. Li, Z.; Jiao, L.; Zhang, B.; Xu, G.; Liu, J. Understanding the Pattern and Mechanism of Spatial Concentration of Urban Land Use, Population and Economic Activities: A Case Study in Wuhan, China. *Geo-Spat. Inf. Sci.* **2021**, *24*, 678–694. [CrossRef]

54. Silverman, B.W. Experimental and Numerical Investigation of an Offset Jet Using Tangential Air Distribution System. *Monogr. Stat. Appl. Probab.* **1986**, *60*, 129–136. [CrossRef]

55. Li, H.; Zhou, Y.; Li, X.; Meng, L.; Wang, X.; Wu, S.; Sodoudi, S. A New Method to Quantify Surface Urban Heat Island Intensity. *Sci. Total Environ.* **2018**, *624*, 262–272. [CrossRef]

56. Anderson, T.K. Kernel Density Estimation and K-Means Clustering to Profile Road Accident Hotspots. *Accid. Anal. Prev.* **2009**, *41*, 359–364. [CrossRef]

57. Zhen, F.; Cao, Y.; Qin, X.; Wang, B. Delineation of an Urban Agglomeration Boundary Based on Sina Weibo Microblog 'Check-in' Data: A Case Study of the Yangtze River Delta. *Cities* **2017**, *60*, 180–191. [CrossRef]

58. Kuang, B.; Lu, X.; Zhou, M.; Chen, D. Provincial Cultivated Land Use Efficiency in China: Empirical Analysis Based on the SBM-DEA Model with Carbon Emissions Considered. *Technol. Forecast. Soc. Change* **2020**, *151*, 119874. [CrossRef]

59. Tang, L.; Liu, M.; Ren, B.; Wu, Z.; Yu, X.; Peng, C.; Tian, J. Sunlight Ultraviolet Radiation Dose Is Negatively Correlated with the Percent Positive of SARS-CoV-2 and Four Other Common Human Coronaviruses in the U.S. *Sci. Total Environ.* **2021**, *751*, 141816. [CrossRef]

60. Bashir, M.F.; Ma, B.; Bilal; Komal, B.; Bashir, M.A.; Tan, D.; Bashir, M. Correlation between Climate Indicators and COVID-19 Pandemic in New York, USA. *Sci. Total Environ.* **2020**, *728*, 138835. [CrossRef]

61. Kowe, P.; Mutanga, O.; Dube, T. Advancements in the Remote Sensing of Landscape Pattern of Urban Green Spaces and Vegetation Fragmentation. *Int. J. Remote Sens.* **2021**, *42*, 3797–3832. [CrossRef]

62. Li, B.; Liu, Y.; Xing, H.; Meng, Y.; Yang, G.; Liu, X.; Zhao, Y. Integrating Urban Morphology and Land Surface Temperature Characteristics for Urban Functional Area Classification. *Geo-Spat. Inf. Sci.* **2022**, *25*, 337–352. [CrossRef]

63. Chen, Y.; Xu, Z.; Byrne, J.; Xu, T.; Wang, S.; Wu, J. Can Smaller Parks Limit Green Gentrification? Insights from Hangzhou, China. *Urban For. Urban Green.* **2021**, *59*, 127009. [CrossRef]

64. Zhuang, Q.; Shao, Z.; Li, D.; Huang, X.; Altan, O.; Wu, S.; Li, Y. Isolating the Direct and Indirect Impacts of Urbanization on Vegetation Carbon Sequestration Capacity in a Large Oasis City: Evidence from Urumqi, China. *Geo-Spat. Inf. Sci.* **2022**, *114*, 103058. [CrossRef]

65. Zhuang, Q.; Shao, Z.; Li, D.; Huang, X.; Cai, B.; Altan, O.; Wu, S. Unequal Weakening of Urbanization and Soil Salinization on Vegetation Production Capacity. *Geoderma* **2022**, *411*, 115712. [CrossRef]

66. Shao, Z.; Sumari, N.S.; Portnov, A.; Ujoh, F.; Musakwa, W.; Mandela, P.J. Urban Sprawl and Its Impact on Sustainable Urban Development: A Combination of Remote Sensing and Social Media Data. *Geo-Spat. Inf. Sci.* **2021**, *24*, 241–255. [CrossRef]